Macroscopic parameters from simulations of pore scale flow

Martin Blunt and Peter King
BP Research Centre, Chertsey Road, Sunbury-on-Thames, Middlesex TW16 7LN, United Kingdom
(Received 30 March 1990)

We simulate two-phase flow in a porous medium, which is represented by random, isotropic two- and three-dimensional networks containing up to 80 000 interconnected pore spaces. The simulations are sufficiently large that macroscopic properties of the flow may be determined. For unstable viscous floods, we show that the displacements are compact with a fractal interface between the fluids. The fractal dimension is found as a function of viscosity ratio. For invasion percolation, where the displacement is controlled by capillary forces, and for viscous fingering, we calculate relative permeabilities in an averaged two-phase Darcy equation, which we show are functions of mean saturation. The relative permeabilities also depend on flow rate, which means that the two-phase Darcy equation is nonlinear, even with microscopic linear Poiseuille flow.

I. INTRODUCTION

Oil in reservoirs occupies the microscopic void space in porous rock. The pore structure is very disordered, consisting of a labyrinthine matrix of interconnected tubes and chambers of different sizes. A cross section through a typical oil-bearing rock is shown in Fig. 1(a). The pore spaces are approximately 10–100 μm across, and are usually occupied by water and oil.

Oil reservoirs may be several kilometers in extent. It is a standard recovery procedure to displace the oil by pumping in another fluid, usually water.

To decide on the most efficient method to recover the oil, the fluid flow in the reservoir under different conditions is modeled by computer simulation. It is of considerable economic importance that the predictions are reliable and accurate. Even with very large computers, the simulation can only resolve the reservoir to the scale of approximately 100 m. A single grid block in the computer model has to represent displacements occurring within millions of pores. The small-scale physics is represented by averaged parameters in differential equations. These parameters are measured experimentally on representative core samples of rock a few centimeters across.

This paper attempts to bridge the gap between the microscopic fluid motion in a random medium and the large-scale displacement behavior. Typical flow rates in reservoirs are very slow, of the order of a few feet a day. Hence, on the pore scale the flow is controlled almost entirely by the capillary forces between immiscible oil and water. However, over large distances viscous and bouyancy forces dominate. This problem is a sophisticated and interesting example of the macroscopic averaging of a disordered dynamical process, where the dominant physical process depends on the scale over which we average. An exact theoretical treatment is too complicated to provide anything other than qualitative results. In an experimental study, it is difficult to probe precisely a range of microscopic flow regimes, as well as measure average properties accurately, especially in a fully three-dimensional system.

We simulate flow in a computer network model of a porous medium. Random networks are used to represent the porous matrix. The small-scale physics is specified exactly, and for networks containing many thousands of pore spaces we can find suitable averaged parameters to describe the macroscopic flow on the scale of centimeters. For unstable viscous floods we show that the displacements are compact with a fractal surface between the fluids. We compute the surface fractal dimension as a function of viscosity ratio. We then show that our results are consistent with the two-phase extension of Darcy's law[1,2] at a fixed capillary number and we discuss the effects of competing viscous and capillary forces, and the circumstances under which the law becomes nonlinear.

Both numerical and experimental network models have attempted to tackle these issues several times before. Some of the first work was performed by Payatakes,[3] with recent research by Koplik and co-workers,[4,5] Chen and Wilkinson,[6,7] Lenormand *et al.*[8–14] and Blunt and King.[15,16] However, these studies have been performed on regular, usually two-dimensional grids, which were insufficiently large for a conclusive determination of macroscopic parameters to be made. We use random, isotropic, two- and three-dimensional networks containing up to 80 000 nodes, which represent systems several centimeters across, from which empirical quantities in Darcy's equation can be calculated.

II. SIMULATION

The pore space is represented by a random network of interconnected voids. In two dimensions points are placed independently at random in a circular region. These are connected to near neighbors by a network of triangles, called the Delaunay triangulation. See Fig. 1(b). The points represent large pore spaces, which contain fluid and the connections are thin tubes. Networks containing up to 80 000 pores have been generated.

In three dimensions a dual lattice, or the Voronoi tessellation is used. Points are placed at random in a sphere. Polyhedra surround each point, and occupy the

 ©1990 The American Physical Society

volume nearer to that point than any other. The vertices of the polyhedra represent the pores and the edges the connections between them. Networks containing up to 50 000 vertices have been used. A two-dimensional Voronoi network is illustrated in Fig. 1(c).

Further details on how the networks are generated are given elsewhere.[17] The Delaunay triangulation of random points is a straightforward and consistent method for producing a disordered isotropic lattice.

In the model porous medium the nodes of the network represent pore spaces of equal volume. The connections are thin tubes of an uncorrelated radius r chosen uniformly from the interval $[r_0(1-\lambda), r_0(1+\lambda)]$, where $1 \geq \lambda \geq 0$.

Fluid flow in the network

We model the flow through the networks using the following assumptions.

(a) All the fluid is considered to be contained in the pores or nodes, but all the pressure drops occur in the tubes between them.

(b) The tubes are filled totally with either invading or displaced fluid, but the pores may contain both fluids.

(c) The two fluids are immiscible. The invading fluid is nonwetting.

(d) The capillary pressure difference across an interface between the two fluids at the entrance of a tube is inversely proportional to the tube radius. The nodes are so wide

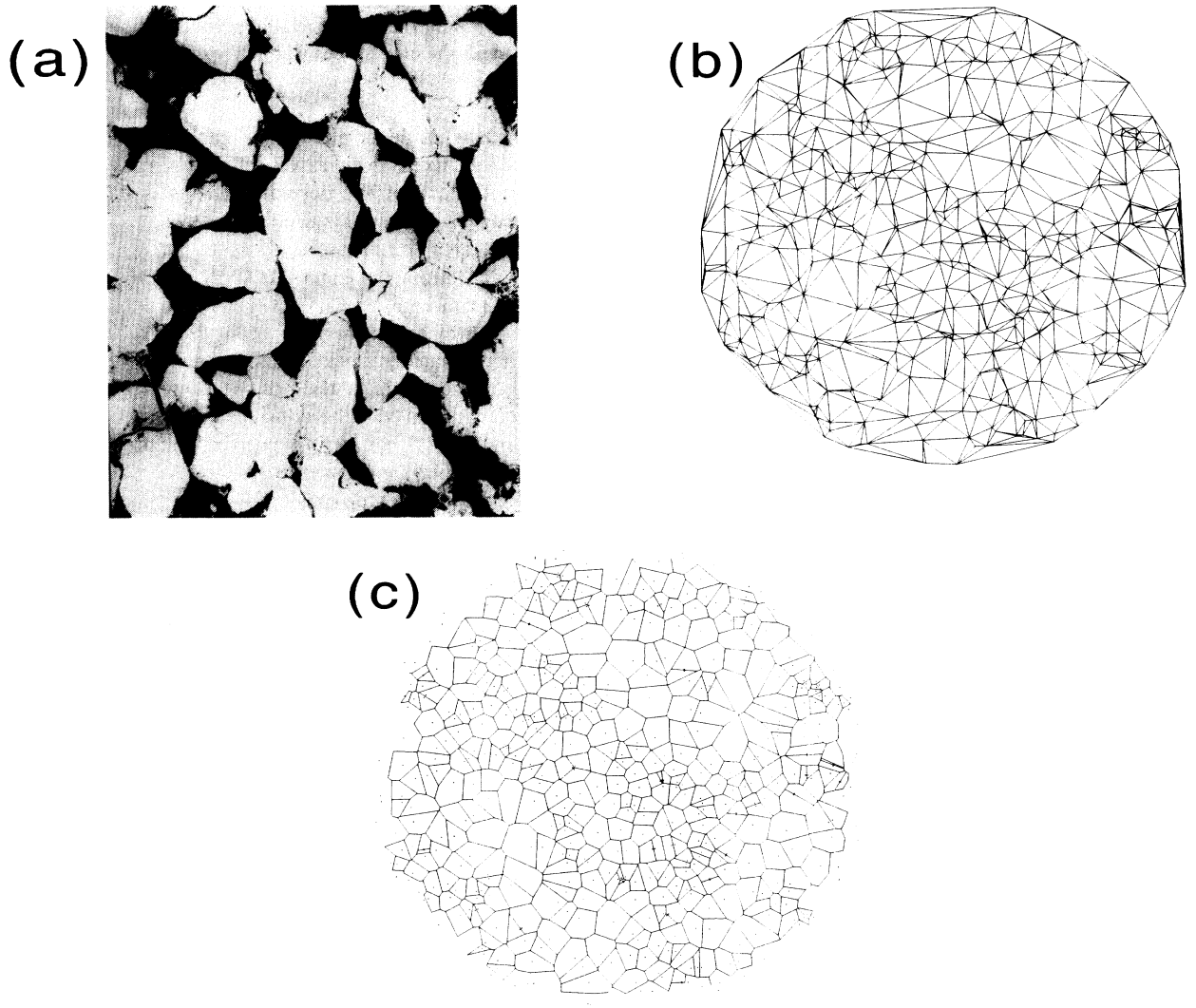

FIG. 1. (a) A cross section through an oil-bearing sandstone magnified 80 times. The pore spaces (dark) in the solid matrix form disordered, interconnected pathways through the rock (light). A typical channel width varies from 10–100 μm. (b) The Delaunay triangulation of 500 points placed at random in a circle. In the simulations a network with 80 000 points is used. The points represent pore spaces and the connections the tubes between them. This network captures the topological disorder of a real porous material, shown in (a), but is not intended as an exact replica. (c) The Voronoi tessellation about 500 points placed in a circle. Three-dimensional analogs containing up to 50 000 vertices were used in the simulations. The vertices represent pore spaces and the edges narrow tubes between them.

that the capillary pressure drop in a node is negligible.

(e) There is Poiseuille flow down each tube.

(f) The fluids are incompressible.

Poiseuille's law for the flow rate Q_{ij} between the tube connecting nodes i and j with no fluid interface in the tube is

$$Q_{ij}=\frac{A(p_i-p_j)r_{ij}^4}{l_{ij}\mu}=g_{ij}\Delta p_{ij} \tag{1}$$

for some constant A, where p is a nodal pressure, r_{ij} and l_{ij} are the radius and length, respectively, of the tube, and μ is the viscosity of the fluid in the tube. In a single node the pressure of the injected and displaced phases are the same and from assumption (b) we model the tubes as being entirely filled with either displaced or injected fluid. If an interface were present in the tube this would introduce a jump in pressure, which would modify Eq. (1). This expression gives a flow rate which is proportional to the local pressure gradient and inversely proportional to the fluid viscosity.

If the fluids are incompressible then $\sum_j Q_{ij}=0$. This enables us to solve for the pressure field p_i using successive over relaxation

$$p_i=\beta\frac{\sum_j g_{ij}p_j}{\sum_j g_{ij}}+(1-\beta)p_i \ , \tag{2}$$

where the sum over j accounts for all nodes connected to node i. The relaxation parameter β is set to 1.7.

We use Eq. (1) to update the volume of injected fluid in the nodes. In a time Δt, a nodal saturation $s_i(t)$ becomes

$$s_i(t+\Delta t)=s_i(t)+\Delta t\sum_j Q_{ij} \ , \tag{3}$$

where the sum only includes bonds connected to node i which contain invaded fluid. Δt is chosen so that only one node in every time step becomes completely filled.

When s_i does reach 1, then bonds connected to node i full of displaced fluid ("empty" bonds) may become full of invaded fluid. An empty bond of radius r_{ij} is filled with invaded fluid if

$$p_i\geq p_j+p_c/r_{ij} \ , \tag{4}$$

where p_c/r_{ij} represents the capillary pressure jump across the fluid interface in a tube, which is inversely proportional to the tube radius. As stated earlier $p_c\geq 0$: the invading fluid is nonwetting. If $p_j+p_c/r_{ij}>p_i\geq p_j$ then the interface is frozen by capillary pressure and no flow occurs across it until p_i increases, i.e.; the conductivity, g_{ij} in Eq. (1) is zero. This is illustrated in Fig. 2.

In some nodes s_i may decrease. If s_i reaches zero, a bond is filled with displaced fluid if $p_i\geq p_j$. Notice that if $p_c=0$ the displaced and invaded fluids are treated symmetrically.

Viscous forces control the fluid fluxes between nodes. The fluid in a tube only changes if the saturation in a node to which it is connected (at either end) rises to 1 or falls to 0.

Initially the network is full of displaced fluid. Nonwetting fluid is injected through a central node. The pressure at this node is chosen at each time step so as to maintain a fixed flow rate. Fluid escapes through the outer boundary of the network, which is held a constant pressure. The scheme is then as follows.

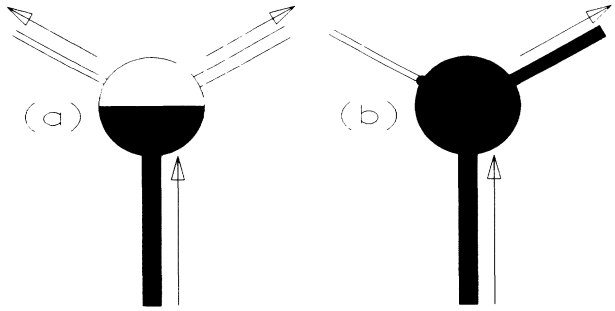

FIG. 2. Diagram showing the saturation update in a single node. (a) Injected (black) fluid is displacing clear fluid. Any pressure jump across the interface in a node is neglected. (b) The node is filled with injected fluid. In viscous fingering any tubes connected to this node will become full of invading fluid, if there is a favorable pressure gradient across it. In invasion percolation only the widest available tube will be filled. The interface in all the other tubes will be frozen.

(a) Solve for the pressure p_i, using Eq. (2).

(b) Calculate a time step Δt such that only one node is filled at a time.

(c) Update the saturations, using Eq. (3).

(d) If the saturation in a node reaches 1 or 0, alter the nature of the fluids in the bonds connected to that node, as described above. The conductivities g_{ij} are recalculated from Eq. (1), or set to zero if the fluid interface is frozen by capillary pressure.

(e) Repeat from step (a).

The balance of viscous to capillary forces is determined by a capillary number N_c. We define N_c to be the ratio of a typical viscous pressure drop across a single tube near the injection site Δp_v to the capillary force p_c/r. From Eq. (1) it can be seen that viscous flows, with a large value of N_c, occur at high flow rates, while at low rates the displacements are governed by capillary forces.

In Ref. 18 this model is used to investigate the flow at a variety of capillary numbers in two-dimensional networks. In this paper three-dimensional results are presented in two extreme limits: viscous fingering when $p_c=0$ or $N_c=\infty$, and invasion percolation, when $N_c=0$. For invasion percolation the algorithm above reduces to simpler growth rules, first described by Chandler *et al.*[19]: at each time step fluid passes through the one available tube with the largest radius and fills up the pore connected to it. An available tube is a tube connecting a pore full of injected fluid to one full of displaced fluid. Since the fluids are incompressible, the flow cannot invade a region of displaced fluid which is completely surrounded and trapped by injected fluid.

III. DISCUSSION OF RESULTS

In viscous fingering capillary forces are neglected. If we inject with a fluid whose viscosity is negligible com-

pared with the other fluid, a very tenuous, wispy pattern is produced. The equations of flow and the structure produced are similar to that found in some aggregation processes.[20] The displacement is extremely ramified and has a fractal geometry.[21] However, at a finite viscosity ratio, which is, of course, the case in all but specially contrived experimental systems, pressure gradients in the injected fluid force the displacement to fill in and a compact structure results, as first shown by Sherwood and Nittmann.[22] The interface between the two fluids is still unstable, however, and a well-developed displacement through a random matrix has a highly convoluted, rough boundary. A measure of this roughness is given by the surface fractal dimension d_s. A smooth surface has a dimension of 2, whereas a fractal is more space filling and has a dimension between 2 and 3. A three-dimensional fingering pattern in a spherical region containing 20 000 nodes is illustrated in Fig. 3(a).

To find the fractal dimension we cover the patterns with a cubic grid of spacing ϵ. A grid block is considered to be occupied if it contains any injected fluid and is empty otherwise. On a cubic lattice each grid block has six nearest neighbors. We compute the number, $N(\epsilon)$, of empty grid blocks which have one or more occupied nearest neighbors. $N(\epsilon)$ is a measure of the apparent surface area of the displacement at a resolution ϵ. We calculate $N(\epsilon)$ as we vary the grid spacing ϵ and find that $N(\epsilon) \sim \epsilon^{-d_s}$ with some noninteger power d_s, which is the fractal dimension of the fluid interface. The fractal dimension is a characterization of the geometry of large patterns.[21] See Fig. 4(a). We can confirm that the bulk of the displacement is compact. As the displacement develops we find the total volume of fluid injected V against the root-mean-square radius r of the pattern. We find $V \sim r^3$, as expected for a filled-in three-dimensional object, Fig. 4(b). Only for displacements at an infinite viscosity ratio is the interior of the displacement fractal,[15,16,20,23] which means that a negligible fraction of the pore space is swept out by the injected fluid. Figure 5 gives approximate values for the surface dimension d_s as a function of viscosity ratio M in two and three dimensions. The results are averaged from three different fingering patterns containing 20 000 nodes of injected fluid at each value of M. Unfortunately, these simulations are insufficiently large for accurate determinations of d_s to be made, since the graphs in Fig. 4 are linear only over a small range of length. In two dimensions the computations of d_s are slightly lower than results on hexagonal networks,[15,16] although they are consistent to within numerical error.

Invasion percolation is the opposite limit: the advance of the fluid interface is controlled entirely by capillary forces.[19,24] Here the injected fluid advances through pathways of wide tubes, bypassing blobs of displaced fluid

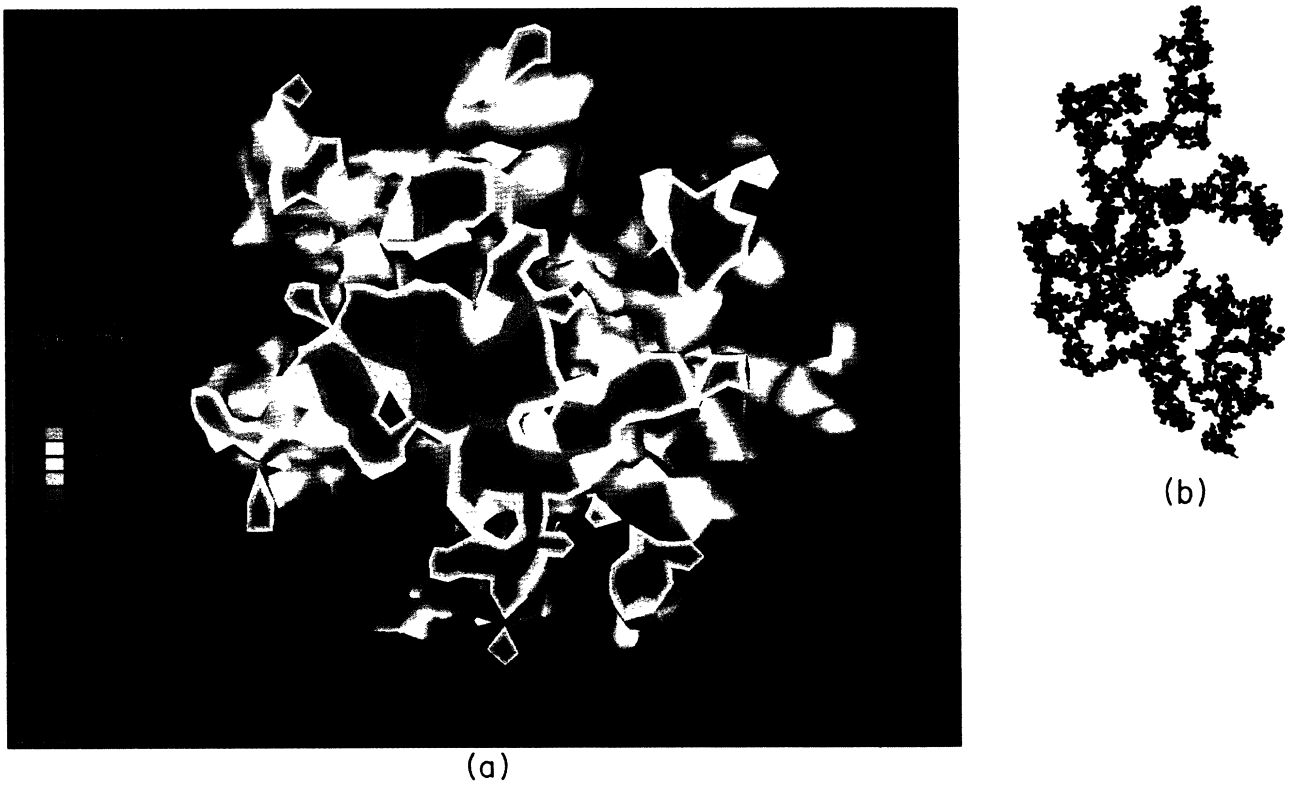

FIG. 3. (a) A three-dimensional viscous fingering pattern. Fluid is injected into the center of a spherical region containing another fluid 100 times more viscous. The contour of 50% saturation of injected fluid is shown. The pattern has been cut through the plane $x=0$ and the colors represent the saturation contours at values greater than 50%. (b) Two-dimensional invasion percolation in a random network of 80 000 nodes.

of all sizes, Fig. 3(b). The process simulates the capillary displacement of a nonwetting fluid at a fixed rate. When the interface first reaches the edge of the network, the displacement pattern is a mass fractal. Unlike a viscous displacement, the pattern is very wispy and does not fill space. The number of grid blocks of size ϵ, $N(\epsilon)$, containing injected fluid scales as ϵ^{-D} with some noninteger power D. D is less than the dimension of space. We find $D=1.82\pm0.01$ in two dimensions and $D=2.44\pm0.05$ in three dimensions. The results are averages from 50 simulations in networks containing 80 000 and 50 000 nodes in two and three dimensions, respectively. These values are consistent with experimental measurements[11] and numerical calculations on regular lattices.[19,24,25] The simulation of invasion percolation continues beyond the time when the invading fluid first reaches the edge of the network (breakthrough) until no further displacement is possible (the terminal point). This occurs when all the displaced fluid is trapped in blobs completely surrounded by injected fluid. In three dimensions this occurs when a finite fraction of the network has been filled by the invader: in two dimensions, however, the breakthrough and terminal times are the same for very large networks.[19]

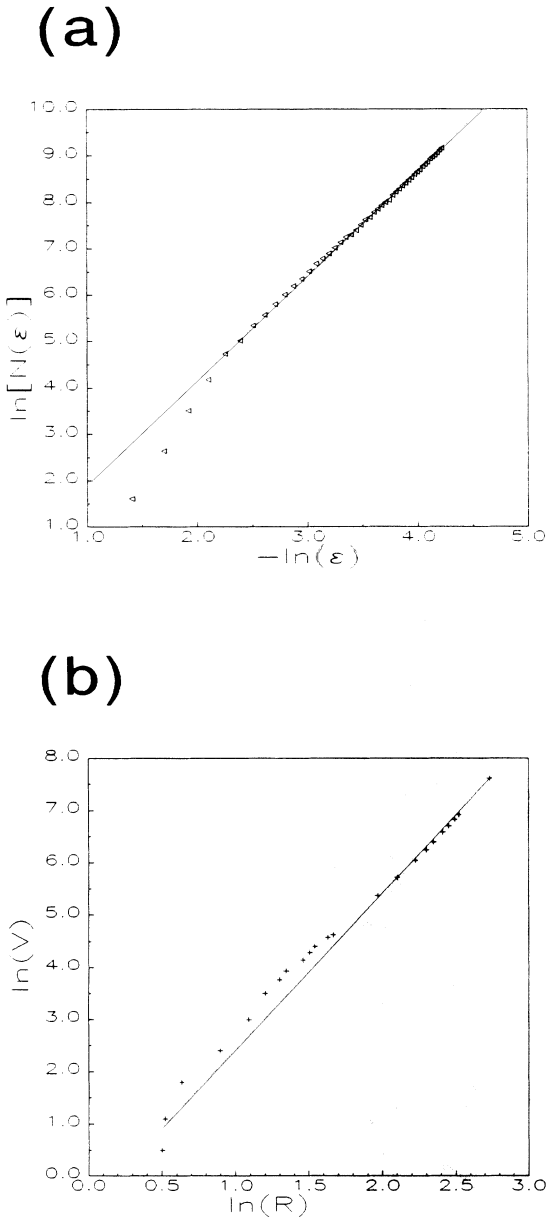

FIG. 4. (a) A doubly logarithmic plot of the apparent surface area $N(\epsilon)$ against grid size ϵ for the fingering displacement illustrated in Fig. 3(a). The graph is an approximate straight line of slope $d_s=2.26\pm0.05$, which is an estimate of the surface dimension of the fluid interface. (b) A doubly logarithmic plot of the volume of injected fluid against root-mean-square radius for the pattern in Fig. 3(a). Here the points lie on a straight line of slope approximately equal to 3, consistent with a compact three-dimensional object.

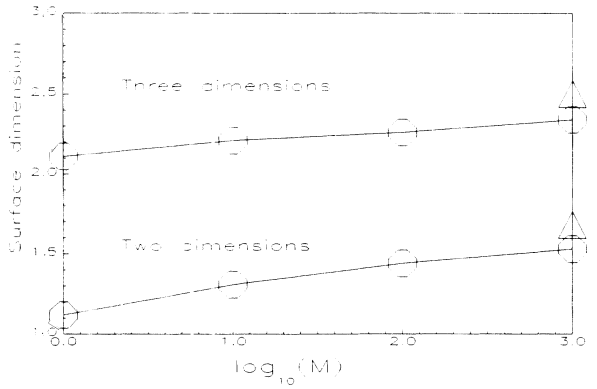

FIG. 5. The dimension of the fluid interface as a function of viscosity ratio M for unstable viscous displacements. The size of the octahedra indicate the statistical error in the computation from different simulations. The triangles represent the calculated dimensions at infinite viscosity ratio, when the displacement is also a mass fractal.

Capillary displacement for fluids with a variety of contact angles, θ ($\theta=180°$ is nonwetting and $\theta=0$ is strongly wetting) has been simulated in two dimensions by Cielpak and Robbins[26] and investigated experimentally by Stokes *et al.* in two and three dimensions.[27,28] They find an invasion percolation like displacement for large contact angles, but show that there is a crossover to a macroscopic frontal advance at a critical contact angle θ_c, when the fluid is partially wetting. In two dimensions the simulations give a fractal dimension $D=1.9$, for $\theta=180°$, which is larger than our value. Their simulation models the displacement at constant pressure, which leads to smaller trapped regions of defending fluid from those seen in invasion percolation, which is a model of a constant rate injection, where the injection pressure may fall if the interface explores regions containing large pores and throats. This could explain why their estimate of D is larger than ours and consistent with D measured from capillary advance without trapping of the defending fluid.[24]

At intermediate capillary numbers, we expect capillary forces to be important at the scale of individual tubes. However, over larger distances, the total viscous pressure

drop will exceed the capillary force and the pattern will look fingered. Invasion percolation is an appropriate model for the microscopic advance, while simulations of viscous fingering indicate the larger structure of the displacement.

IV. MACROSCOPIC PARAMETERS

We have given a quantitative description of the geometry of the displacements. This characterization does not lead easily to a complete and useful description of the dynamics of large floods. For this, another, more conventional, approach is needed. First we consider the flow of a single fluid in a porous medium. If we have Poiseuille flow through each channel, then from Eq. (1) we see that the flow rate is proportional to the pressure gradient and inversely proportional to the fluid viscosity. We would expect the same qualitative behavior if we averaged the flow rate in a representative volume containing many individual pore spaces and connections. This leads to Darcy's law:[1,2]

$$\mathbf{q}=-\frac{K}{\mu}\nabla p \ , \tag{5}$$

where $\mathbf{q}$ is a flow velocity, and K is the absolute permeability.

If there are two fluids flowing, we need a generalization of the Darcy law above, which was first proposed by Muskat:[29,30]

$$\mathbf{q}_i=-K\frac{k_{ri}(s)}{\mu_i}\nabla p_i \ , \tag{6a}$$

$$\mathbf{q}_d=-K\frac{k_{rd}(s)}{\mu_d}\nabla p_d \ , \tag{6b}$$

where the subscripts i and d label the injected and displaced fluids, respectively. The saturation s is defined as the fraction of the total void space occupied by the injected fluid in the volume over which we take the average. This volume is a small section of a larger displacement, but is still of macroscopic size. Through it run fluxes of both injected and displaced fluids. If there are no capillary forces $p_i=p_d$, otherwise $p_i=p_d+P_c$, where P_c is a macroscopic capillary pressure. In this paper we will only present calculations of relative permeability and leave a discussion of this capillary pressure for further studies.

On the microscopic level the fluids occupy separate interpenetrating networks, with flow in tubes between the two fluids inhibited by capillary pressure. Hence the flow rates are reduced from the single phase value by a factor k_r which is called the relative permeability. The relative permeabilities depend on which portions of the void space are occupied by the two fluids. At low flow rates, the flow is dominated by capillary forces and the nonwetting fluid occupies the wider tubes, while much of the displaced fluid resides in disconnected blobs, which do not contribute to the flow. At higher flow rates or if we average on large scales, the advancing front of injected fluid is affected by viscous forces, and k_r takes account of fingering on the averaged fluid velocity. This may be the case in some experimental measurements on rock samples, and is certainly true for relative permeabilities which are used in reservoir simulators. Here more of the channels are accessible to flow and less displaced fluid is bypassed completely.

Three major assumptions have been made to introduce these equations.

(1) That for an experiment with fixed physical properties, such as the capillary number N_c and viscosity ratio M, the relative permeability is a function only of the saturation s. However, k_r could depend on the overall size of the displacement or be largely independent of an average saturation and be controlled by pore-scale properties.

(2) That this computed relative permeability should imply the same saturation profile as the saturations actually observed.

(3) It is often considered that k_r does not depend on N_c, or the length scale l over which we take the average. However, we will show that k_r is a function of capillary number. Experimentally relative permeabilities are usually measured at very low flow rates. At higher capillary numbers, where viscous forces become important, the relative permeability is known to change.[31]

As well as the relative permeabilities, we calculate the fractional flow, F, which is the fraction of the total flow $\mathbf{q}_t=\mathbf{q}_i+\mathbf{q}_d$ carried by the injected fluid. For a purely viscous flood, $F=\mu_d k_{ri}(s)/[\mu_i k_{rd}(s)+\mu_d k_{ri}(s)]$, which is assumed to be a function of saturation only.

Our microscopic simulation can be used to test the validity of the three assumptions outlined above.

The average pressures, saturations, and flow rates are computed at various times throughout the simulation in forty annular regions dividing our spherical and circular networks. This represents an average between 500 and 2000 individual pore spaces. Example results for a purely viscous displacement are shown in Fig. 6, where the fractional flow calculated at over ten times during the growth in three different simulations is plotted against the mean saturation. Notice that the points lie on a single curve, which is required by the empirical description, although it is not imposed by the pore-scale physics. This verifies the first assumption we made above.

We will now demonstrate that this fractional flow is consistent with the observed average saturation profile, the two-phase Darcy equations, and the conservation of fluid for viscous floods in three dimensions. For incompressible fluids conservation requires that $\nabla\cdot\mathbf{q}_t=0$. For simple radial flow the solution is $q_t=q_0/r^2$, where r is the distance from the injection site. The conservation equation for the injected fluid is

$$\frac{\partial s}{\partial t}+\nabla\cdot\mathbf{q}_i=0 \ . \tag{7}$$

For a viscous flood ($N_c=\infty$), $\mathbf{q}_i=F(s)\mathbf{q}_t$. Then we take the annular average of Eq. (7), so that the saturation s is a function of r and t only:

$$\frac{\partial s(r,t)}{\partial t}+\frac{1}{r}\frac{\partial}{\partial r}[q_0F(s(r,t))]=0 \ . \tag{8}$$

Equation (8) can be written in terms of the single variable $v=r/(3q_0t)^{1/3}$:

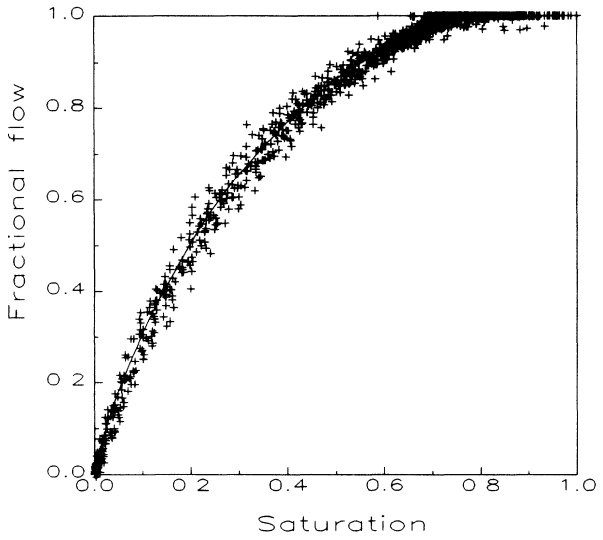

FIG. 6. The fractional flow of injected fluid as a function of local mean saturation. The points are direct calculations in forty annular regions of the network taken at over ten stages during the flood from three different simulations of three-dimensional viscous fingering with $M=10$. Notice that the points all lie on a single curve. The solid line is the fractional flow, which from the solution of the two-phase Darcy equations would give the average saturation profile which is actually observed.

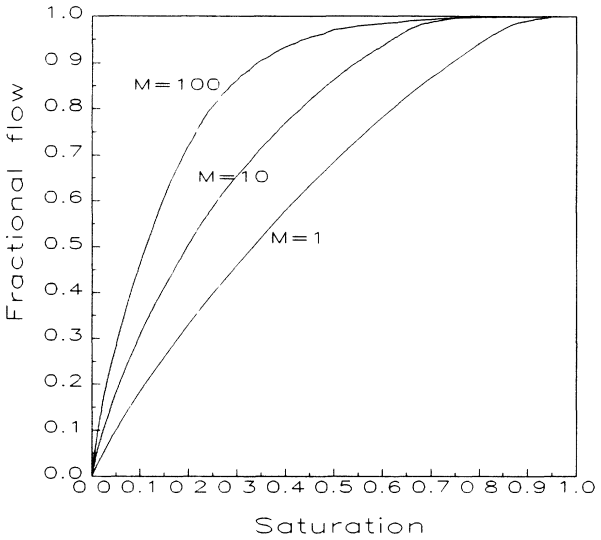

FIG. 7. Fractional flow curves for three-dimensional viscous fingering. The viscosity ratio M is indicated on the figure. The curves are obtained from integrating the mean saturation profile as described in the text.

$$\frac{ds}{dv}\left[v^3-\frac{dF(s)}{ds}\right]=0\ . \tag{9}$$

Hence once $s(v)$ is known, the consistent fractional flow is simply

$$F(s)=\int_0^s v^3(s)ds\ . \tag{10}$$

The computed saturation profiles s are functions only of v for fixed M and N_c. Equation (10) is used to find $F(s)$ which is the solid curve in Fig. 6. Our two independent determinations of $F(s)$ yield the same function. This supports assumption (2).

Figure 7 shows fractional flow curves for a variety of viscosity ratios. The larger the viscosity ratio M, the greater the degree of fingering and the fractional flow departs further from the near linear function seen for $M=1$. The fractional flow is not exactly $F(s)=s$ for $M=1$ since the network is inhomogeneous. There is some irregularity in the fluid interface, and a small fraction of the displaced fluid is trapped in small blobs containing one or two nodes. We have verified that $F(s)$ determined from Eq. (10) and the directly computed values are consistent for each value of M.

The relative permeability can also be found directly using Eq. (6), and example curves for purely viscous and purely capillary floods in three dimensions are shown in Fig. 8. Notice that for the capillary flood, the relative permeability of the displaced fluid reaches zero when only 36% of the pores are filled, which means that 64% of them are occupied by trapped, immobile regions surrounded by the injected fluid. In the viscous displacement a much lower fraction of displaced fluid is bypassed.

The relative permeabilities in Fig. 8 are not the same and hence k_r is a function of capillary number. Assumption (3) is not correct. In dynamic situations the relative permeability depends on the microscopic balance of viscous to capillary forces, which controls the network of pores and throats through which the fluids flow. k_r may also be affected by the total viscous pressure drop across the volume over which we average, since this determines the overall movement of the displacement. Thus relative

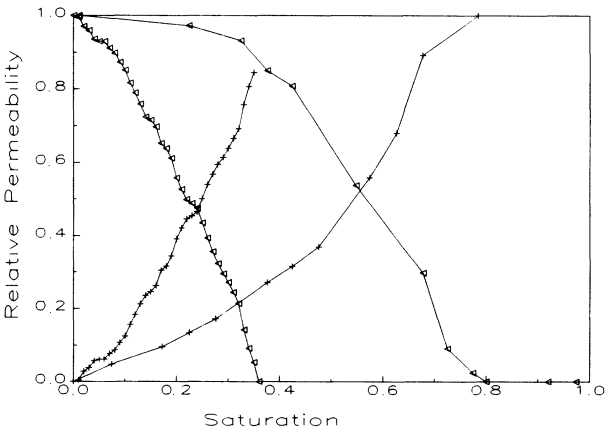

FIG. 8. Relative permeabilities as a function of saturation computed on a three-dimensional network. Crosses, injected fluid; triangles, displaced fluid. The curves to the left are for capillary dominated flows and on the right are for a viscous fingering pattern with $M=10$. The relative permeability is an empirical macroscopic function, which controls the motion of large displacements through the Darcy equation.

permeabilities measured at low flow rates on small core samples may not be the same as those which will govern the macroscopic behavior in oil reservoirs, where viscous forces are significant. The appropriate manner in which relative permeability should be used in the prediction of the flow in large systems, or in cases with different capillary numbers, should be the subject of further work. The concept of relative permeability is subtle, but still of considerable use for the description of large displacements.

Relative permeabilities are measured experimentally in systems where the microscopic flow mechanisms are not known. We have been able to derive a macroscopic computation in a system where the microscopic physics is precisely specified. This demonstrates that the simple physical mechanisms of pore-scale movement are consistent with an averaged Darcy law description at a fixed capillary number. Despite several analytical approaches,[32–35] this has not been achieved directly before.

V. CONCLUSIONS

We have used a network model of flow in a random porous medium to study the effect of viscous and capillary forces on pore-scale displacements in both two and three dimensions. We described the fractal geometry of viscous and capillary dominated floods.

The linear microscopic flow dynamics in our model is well defined. The macroscopic displacement behavior is conventionally described by the two-phase Darcy law, which introduces empirical relative permeability and fractional flow functions. We computed these quantities, showed that they are functions of local saturation, and demonstrated that they are consistent with the observed radial saturation profile. The model can be used to identify the physical parameters on which the relative permeability depends. We have shown the relative permeabilities for extremely high and low flow rates. In a flow with competing viscous and capillary forces across the length over which we take the average, the relative permeability will lie between these extremes, and will be a function of both flow rate and length scale, which leads to a nonlinear averaged Darcy equation.

ACKNOWLEDGMENTS

We are grateful for Dr. P. K. Sweby and Dr. J. J. Barley for providing us with programs to generate the random networks illustrated in Fig. 1.

[1]M. Darcy, *Les Fontaines Publiques de la Ville de Dijon* (Dalmont, Paris, 1856).
[2]A. E. Scheidegger, *The Physics of Flow through Porous Media* (University of Toronto Press, Toronto, 1974).
[3]A. C. Payatakes, Ann. Rev. Fluid Mech. **14**, 365 (1982).
[4]J. Koplik and T. J. Lasseter, Chem. Eng. Commun. **26**, 285 (1984).
[5]J.-D. Chen and J. Koplik, J. Colloid Interface Sci. **108**, 304 (1985).
[6]J.-D. Chen and D. Wilkinson, Phys. Rev. Lett. **55**, 1892 (1985).
[7]J.-D. Chen, J. Colloid Interface Sci. **110**, 488 (1986).
[8]R. Lenormand, E. Touboul, and C. Zarcone, J. Fluid Mech. **189**, 165 (1988).
[9]R. Lenormand, Proc. R. Soc. London, Ser. A **423**, 159 (1989).
[10]R. Lenormand and C. Zarcone, in *Proceedings of the Fifty-Ninth Annual Technical Conference and Exhibition of the Society of Petroleum Engineers, Houston, Texas, 1984* (Society of Petroleum Engineers, Texas, 1984), SPE 13264.
[11]R. Lenormand and C. Zarcone, Phys. Rev. Lett. **54**, 2226 (1985).
[12]R. Lenormand, in *Proceedings of the Fifth Symposium on Enhanced Oil Recovery, Tulsa, Oklahoma, 1986* (Society of Petroleum Engineers, Texas, 1986), SPE 14882, pp. 23-31.
[13]R. Lenormand, Physica A **140**, 114 (1986).
[14]R. Lenormand and C. Zarcone, Transp. Porous Media **4**, 599 (1989).
[15]P. R. King, J. Phys. A **20**, L529 (1987).
[16]M. J. Blunt and P. R. King, Phys. Rev. A **37**, 3935 (1988).
[17]M. J. Blunt, J. A. Goshawk, P. R. King, and R. C. Ball (unpublished); M. Sever, COMPEL—Int. J. Comput. Math. Electr. Electron. Eng. **5**, 75 (1986).
[18]M. J. Blunt and P. R. King, Transp. Porous Media (to be published).
[19]R. Chandler, J. Koplik, K. Lerman, and J. F. Willemsen, J. Fluid Mech. **119**, 249 (1982).
[20]L. Paterson, Phys. Rev. Lett. **52**, 1621 (1984).
[21]B. B. Mandelbrot, *The Fractal Geometry of Nature* (Freeman, San Francisco, 1982).
[22]J. D. Sherwood and J. Nittmann, J. Phys. **47**, 15 (1986).
[23]J. Nittmann, G. Daccord, and H. E. Stanley, Nature **314**, 141 (1985).
[24]D. Wilkinson and J. F. Willemsen, J. Phys. A **16**, 3365 (1983).
[25]L. Furuberg, J. Feder, A. Aharony, and T. Jøssang, Phys. Rev. Lett. **61**, 2117 (1988).
[26]M. Cielpak and M. O. Robbins, Phys. Rev. Lett. **60**, 2042 (1988).
[27]J. P. Stokes, D. A. Weitz, J. P. Gollub, A. Dougherty, M. O. Robbins, P. M. Chaikin, and H. M. Lindsay, Phys. Rev. Lett. **57**, 1718 (1986).
[28]J. P. Stokes, A. Kushnick, and M. O. Robbins (unpublished).
[29]M. Muskat and M. W. Meres, Physics **7**, 346 (1936).
[30]D. W. Peaceman, *Fundamentals of Numerical Reservoir Simulation* (Elsevier, Amsterdam, 1977).
[31]F. A. L. Dullien, *Porous Media. Fluid Transport and Pore Structure* (Academic, New York, 1979).
[32]A. E. Scheidegger, J. App. Phys. **25**, 994 (1954).
[33]S. Levine and D. L. Cutheill, J. Can. Pet. Technol. **25**, 74 (1986).
[34]S. Whitaker, Transp. Porous Media **1**, 3 (1986).
[35]P. M. Adler and H. Brenner, Ann. Rev. Fluid Mech. **20**, 35 (1988).

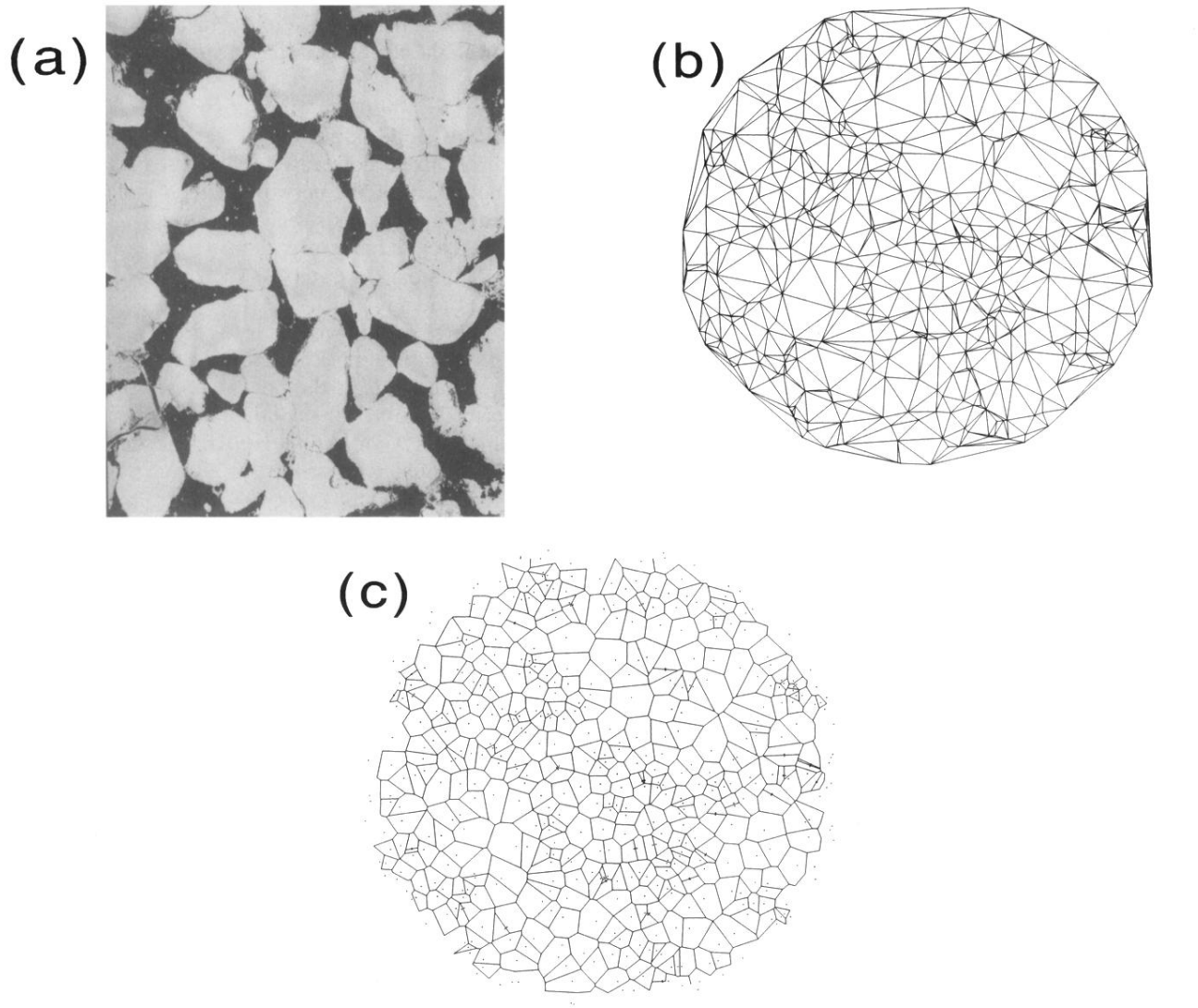

FIG. 1. (a) A cross section through an oil-bearing sandstone magnified 80 times. The pore spaces (dark) in the solid matrix form disordered, interconnected pathways through the rock (light). A typical channel width varies from 10–100 μm. (b) The Delaunay triangulation of 500 points placed at random in a circle. In the simulations a network with 80 000 points is used. The points represent pore spaces and the connections the tubes between them. This network captures the topological disorder of a real porous material, shown in (a), but is not intended as an exact replica. (c) The Voronoi tessellation about 500 points placed in a circle. Three-dimensional analogs containing up to 50 000 vertices were used in the simulations. The vertices represent pore spaces and the edges narrow tubes between them.

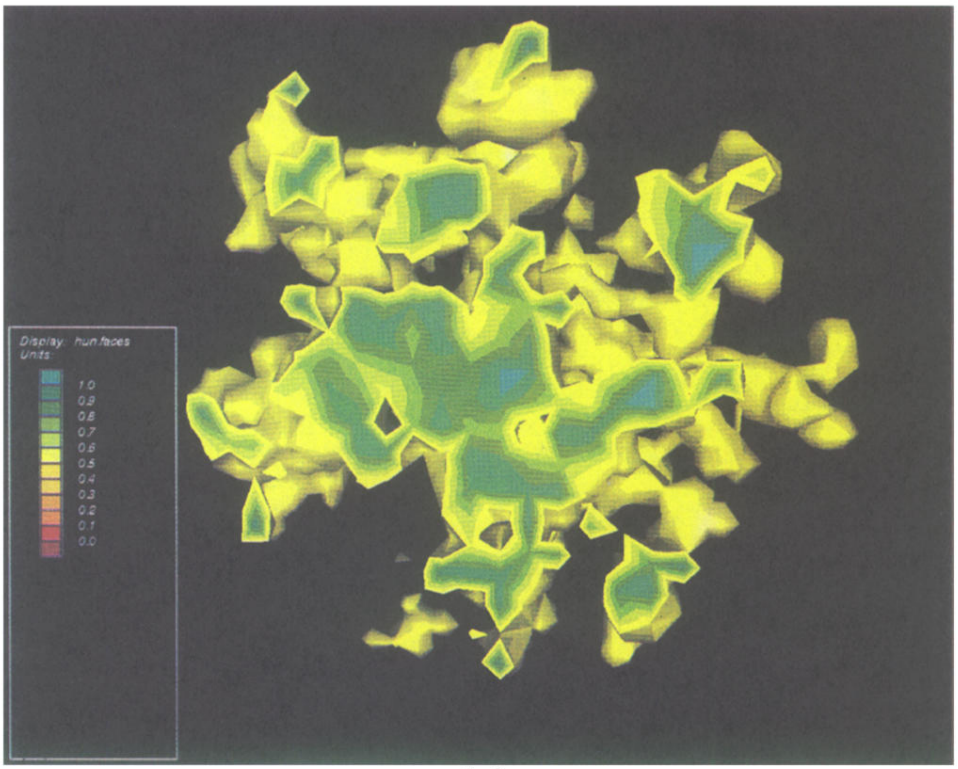

(a)

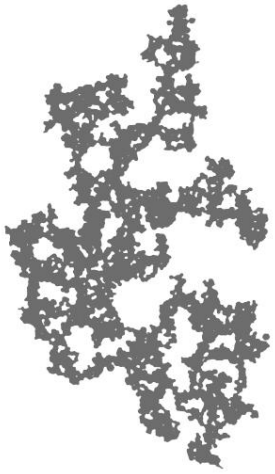

(b)

FIG. 3. (a) A three-dimensional viscous fingering pattern. Fluid is injected into the center of a spherical region containing another fluid 100 times more viscous. The contour of 50% saturation of injected fluid is shown. The pattern has been cut through the plane $x=0$ and the colors represent the saturation contours at values greater than 50%. (b) Two-dimensional invasion percolation in a random network of 80 000 nodes.